8.1: ENDOR

Advantages of electron-spin based detection of nuclear frequency spectra

Nuclear frequency spectra in the liquid (Section 4.3.2) and solid states (4.3.4) exhibit much better hyperfine resolution than EPR spectra, because the former spectra feature fewer and narrower lines. In fact, small hyperfine couplings to ligand nuclei in metal complexes are not usually resolved in EPR spectra and only the largest hyperfine couplings may be resolved in solid-state EPR spectra. The nuclear frequency spectra cannot be measured by a dedicated NMR spectrometer because they extend over several Megahertz to several tens of Megahertz, whereas NMR spectrometers are designed for excitation and detection bandwidths of a few tens of kilohertz. Furthermore, electron spin transitions have 660 times more polarization than proton transitions and more than that for other nuclei. Their larger magnetic moment also leads to higher detection sensitivity. It is thus advantageous to transfer polarization from electron spins to nuclear spins and to backtransfer the response of the nuclear spins to the electron spins for detection. Two classes of experiments can achieve this, electron nuclear double resonance (ENDOR) experiments, discussed in Section *[Math Processing Error]* and electron spin echo envelope modulation (ESEEM) experiments discussed in Section 8.2.

Types of ENDOR experiments

An ENDOR experiment can be performed with strong CW irradiation of both electron and nuclear spins. In this CW ENDOR experiment, an electron spin transition is partially saturated, *[Math Processing Error]* in Eq. (7.5). By driving a nuclear spin transition that shares an energy level with the saturated transition, additional relaxation pathways are opened up. The electron spin transition under observation is thus partially desaturated, and an increase in the EPR signal is observed. The experiment is performed at constant magnetic field with strong microwave irradiation at a maximum of the first-derivative absorption spectrum (i.e. the CW EPR spectrum) and the EPR signal is recorded as a function of the frequency of additional radiofrequency irradiation, which must fulfill the saturation condition *[Math Processing Error]* for the nuclear spins. Usually, the radiofrequency irradiation is frequency modulated and the response is detected with another phase-sensitive detector, which leads to observation of the first derivative of the nuclear frequency spectrum. The CW ENDOR experiment depends critically on a balance of relaxation times, so that in the solid state sufficient sensitivity may only be achieved in a certain temperature range. Furthermore, simultaneous strong continuous irradiation by both microwave and radiofrequency, while keeping resonator frequency and temperature constant, is experimentally challenging. Therefore, CW ENDOR has been largely replaced by pulsed ENDOR techniques. However, for liquid solution samples CW ENDOR is usually the only applicable ENDOR technique.

The conceptually simplest pulsed ENDOR experiment is Davies ENDOR (Section 8.1.3), where saturation of the EPR transition is replaced by inversion by a *[Math Processing Error]* pulse (Fig. 8.1(a)). A subsequent radiofrequency *[Math Processing Error]* pulse, which is on-resonant with a transition that shares a level with the inverted EPR transition, changes population of this level and thus polarization of the EPR observer transition. This polarization change as a function of the radiofrequency is observed by a Hahn echo experiment on the observer transition. The approach works well for moderately large hyperfine couplings *[Math Processing Error]*, in particular for *[Math Processing Error]* nuclei directly coordinated to a transition metal ion or for protons at hydrogen-bonding distance or distances up to about *[Math Processing Error]*. As we shall see in Section 8.1.3, the experiment is rather insensitive for very small hyperfine couplings.

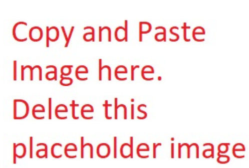

Figure 8.1: Pulsed ENDOR sequences. (a) Davies ENDOR. A selective inversion *[Math Processing Error]* pulse on the electron spins is followed by a delay *[Math Processing Error]* and Hahn echo detection (red). During microwave interpulse delay *[Math Processing Error]*, a frequency-variable radiofrequency *[Math Processing Error]* pulse is applied (blue). If this pulse is on resonant with a nuclear transition, the inverted echo recovers (pale blue). (b) Mims ENDOR. An non-selective stimulated echo sequence with interpulse delays *[Math Processing Error]* and *[Math Processing Error]* is applied to the electron spins (red). During microwave interpulse delay *[Math Processing Error]*, a frequency-variable radiofrequency *[Math Processing Error]* pulse is applied (blue). If this pulse is on resonant with a nuclear transition, the stimulated echo is attenuated (pale blue).

The smallest hyperfine couplings can be detected with the Mims ENDOR experiment that is based on the stimulated echo sequence *[Math Processing Error]* Fig. *[Math Processing Error]* b) *[Math Processing Error]*). The preparation block *[Math Processing Error]* creates a polarization grating of the functional form *[Math Processing Error]*, where *[Math Processing Error]* is the EPR absorption spectrum as a function of the resonance offset *[Math Processing Error]* and *[Math Processing Error]* is the delay between the two *[Math Processing Error]* microwave pulses. A radiofrequency *[Math Processing Error]* pulse with variable frequency is applied during time *[Math Processing Error]* when the electron spin magnetization is aligned with the *[Math Processing Error]* axis. If this pulse is on resonant with a nuclear transition that shares a level with the observer EPR transition, half of the polarization grating is shifted by the hyperfine splitting *[Math Processing Error]*, as will also become apparent in Section 8.1.3. For *[Math Processing Error]* with integer *[Math Processing Error]* the polarization grating is destroyed by destructive interference. Since the stimulated echo is the free induction decay (FID) of this polarization grating, it is canceled by a radiofrequency pulse that is on resonant with a nuclear transition. It is apparent that the radiofrequency *[Math Processing Error]* pulse has no effect for *[Math Processing Error]* with integer *[Math Processing Error]*, where the original and frequency-shifted gratings interfere constructively. Hence, the Mims ENDOR experiment features blind spots as a function of interpulse delay *[Math Processing Error]*. These blind spots are not a serious problem for very small hyperfine couplings *[Math Processing Error]*. Note however that the first blind spot corresponds to *[Math Processing Error]*. Hence, long interpulse delays *[Math Processing Error]* are required in order to detect very small hyperfine couplings, and this leads to strong echo attenuation by a factor *[Math Processing Error]* due to electron spin transverse relaxation. It can be shown that maximum sensitivity for very small couplings is attained approximately at *[Math Processing Error]*.

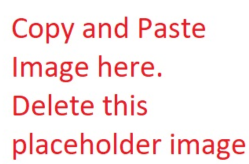

Figure 8.2: Polarization transfer in Davies ENDOR. (a) Level populations at thermal equilibrium, corresponding to green label 0 in Fig. 8.1(a). The electron transitions (red, pale red) are much more strongly polarized than the nuclear transitions (blue, pale blue). (b) Level populations after a selective mw inversion pulse on resonance with the *[Math Processing Error]* transition (dark red), corresponding to green label 1 in Fig. 8.1(a). A state of two-spin order is generated, where the two electron spin transitions are polarized with opposite sign and the same is true for the two nuclear spin transitions. (c) Level populations after a selective rf inversion pulse on resonance with the *[Math Processing Error]* transition (dark blue), corresponding to green label 2 in Fig. 8.1(a). The electron spin observer transition *[Math Processing Error]* is no longer inverted, but only saturated.

Davies ENDOR

The Davies ENDOR experiment is most easily understood by looking at the polarization transfers. At thermal equilibrium the electron spin transitions (red and pale red) are much more strongly polarized than the nuclear spin transitions (Fig. 8.2(a)). Their frequencies differ by an effective hyperfine splitting *[Math Processing Error]* to a nuclear spin *[Math Processing Error]* that is color-coded blue. The first microwave *[Math Processing Error]* pulse is transition-selective, i.e., it has an excitation bandwidth that is smaller than *[Math Processing Error]*. Accordingly, it inverts only one of the two electron spin transitions. We assume that the *[Math Processing Error]* transition (red) is inverted and the *[Math Processing Error]* transition (pale red) is not inverted; the other case is analogous. Such transition-selective inversion leads to a state of two-spin order, where all individual transitions in the two-spin system are polarized. However, the two electron spin transitions are polarized with opposite sign and the two nuclear transitions are also polarized with opposite sign (Fig. 8.2(b)). Now a radiofrequency *[Math Processing Error]* pulse is applied. If this pulse is not resonant with a nuclear transition, the state of two-spin order persists and the observer electron spin transition (red) is still inverted. The radiofrequency pulse is also transition-selective. We now assume that this pulse inverts the *[Math Processing Error]* transition (blue); the other case is again analogous. After such a resonant radiofrequency pulse, the two nuclear transitions are polarized with equal sign and the two electron spin transitions are saturated with no polarization existing on them (Fig. 8.2(c)). After the radiofrequency *[Math Processing Error]* pulse a microwave Hahn echo sequence is applied resonant with the observer transition (Fig. 8.1(a)). If the radiofrequency pulse was off resonant (situation as in Fig. 8.2(b)), an inverted echo is observed. If, on the other hand, the radiofrequency pulse was on resonant (situation as in Fig. 8.2(c)) no echo is observed. In practice, polarization transfers are not complete and a weak echo is still observed. However, an on-resonant radiofrequency pulse causes some recovery of the inverted echo. If the radiofrequency is varied, recovery of the inverted echo is observed at all frequencies where the radiofrequency pulse is resonant with a nuclear transition.

Figure 8.3: Spectral hole burning explanation of Davies ENDOR. (a) An inhomogeneously broadened EPR line with width *[Math Processing Error]* (red) consists of many narrower homogeneously broadened lines with linewidth *[Math Processing Error]*. (b) Long weak microwave irradiation saturates the on-resonant spin packet and does not significantly affect off-resonant spin packets. A spectral hole is burnt into the inhomogeneously broadened line, which can be as narrow as *[Math Processing Error]*. (c) A selective microwave *[Math Processing Error]* pulse burns an inversion hole into the EPR line whose width is approximately the inverse width of the pulse. (d) Situation after applying an on-resonant radiofrequency pulse. For the spin packet, where the microwave pulse was on-resonant with the *[Math Processing Error]* transition, half of the spectral hole is shifted by *[Math Processing Error]* to lower EPR frequencies. For the spin packet where the microwave pulse was on-resonant with the *[Math Processing Error]* transition, half of the spectral hole is shifted by *[Math Processing Error]* to higher EPR frequencies. Considering both cases, half of the hole persists, corresponding to saturation. Two side holes with a quarter of the depth of the inversion hole are created at *[Math Processing Error]*. These side holes do not contribute to the echo signal, as long as they are outside the detection window (pale red) whose width is determined by the excitation bandwidth of the Hahn echo detection sequence.

Further understanding of Davies ENDOR is gained by considering an inhomogeneously broadened EPR line (Fig. 8.3). In such a line with width *[Math Processing Error]*, each individual spin packet with much narrower width *[Math Processing Error]* can, in principle, be selectively excited. A long rectangular *[Math Processing Error]* pulse inverts the on-resonant spin packet and partially inverts spin packets roughly over a bandwidth corresponding to the inverse length of the pulse. In Davies ENDOR, pulse lengths between 50 and *[Math Processing Error]*, corresponding to excitation bandwidths between 20 and *[Math Processing Error]* are typical. Such a pulse creates an inversion hole centered at the microwave frequency *[Math Processing Error]*. In an *[Math Processing Error]* electron-nuclear spin system, two on-resonant spin packets exist, those where *[Math Processing Error]* is the frequency of the *[Math Processing Error]* transition and those where it is the frequency of the *[Math Processing Error]* transition. For the former spin packet, inversion of the nuclear spin from the *[Math Processing Error]* to the *[Math Processing Error]* state increases the EPR frequency by the effective hyperfine splitting *[Math Processing Error]*, whereas for the latter packet, inversion from the *[Math Processing Error]* to the *[Math Processing Error]* state decreases it by *[Math Processing Error]*. In both cases half of the inversion hole is shifted to a side hole, leaving a saturation hole at *[Math Processing Error]* and creating a saturation side hole. The saturation center holes of the two spin packets coincide in frequency and combine to a saturation hole in the inhomogeneously broadened line. At the side hole frequencies *[Math Processing Error]*, only one of the two spin packets contributes to the hole, so that the side holes are only half as deep. The Hahn echo subsequence in the Davies ENDOR sequence must have a detection bandwidth that covers only the central hole (pale red in Fig. *[Math Processing Error]*), since no ENDOR effect would be observed if the side hole would also be covered. For this purpose, the detection bandwidth of the Hahn echo sequence can be limited either by using sufficiently long microwave pulses or by using a sufficiently long integration gate for the inverted echo.

In any case, a Davies ENDOR effect is only be observed if *[Math Processing Error]* exceeds the width of the original inversion hole. The smaller *[Math Processing Error]*, the longer the first inversion pulse needs to be and the fewer spin packets contribute to the signal. In general, hyperfine splittings much smaller than the homogeneous linewidth *[Math Processing Error]* in the EPR spectrum cannot be detected. In practice, Davies ENDOR becomes very insensitive for *[Math Processing Error]* pulse lengths exceeding 400 ns. If broadening of the inversion hole by electron spin relaxation is negligible, the suppression of signals with small hyperfine couplings in Davies ENDOR can be described by a selectivity parameter

[Math Processing Error]

where *[Math Processing Error]* the length of the first mw *[Math Processing Error]* pulse. Maximum absolute ENDOR intensity *[Math Processing Error]* is obtained for *[Math Processing Error]*. As a function of *[Math Processing Error]*, the absolute ENDOR intensity is given by

[Math Processing Error]

The hyperfine contrast selectivity described by Eq. (8.2) can be used for spectral editing. For instance, *[Math Processing Error]* ENDOR signals of directly coordinated ligand nitrogen atoms in transition metal complexes with *[Math Processing Error]* of the order of *[Math Processing Error]* overlap with *[Math Processing Error]* ENDOR signals of weakly coupled ligand protons at X-band frequencies. At an inversion pulse length of about *[Math Processing Error]* ENDOR signals are largely suppressed.

The sensitivity advantage of Mims ENDOR for very small hyperfine couplings can also be understood in the hole burning picture. Instead of a single center hole, a preparation block *[Math Processing Error]* with nonselective microwave pulses creates a polarization grating that can be imagined as a comb of many holes that are spaced by frequency difference *[Math Processing Error]*. The width of each hole is approximately *[Math Processing Error]*. The width of the comb of holes is determined by the inverse length of the non-selective *[Math Processing Error]* pulses, which are typically *[Math Processing Error]* long. For small couplings, where *[Math Processing Error]* in Davies ENDOR needs to be very long, more than an order of magnitude more spin packets take part in a Mims ENDOR experiment than in a Davies ENDOR experiment. The Mims ENDOR effect arises from the shift of one quarter of the polarization grating by frequency difference *[Math Processing Error]* and one quarter of the grating by *[Math Processing Error]*. The shifted gratings interfer with the grating at the center frequency. Depending on *[Math Processing Error]* and on the periodicity *[Math Processing Error]* of the grating, this interference is destructive (ENDOR effect) or constructive (no ENDOR effect).